DOE/ET-53088-**294(R)** IFSR #**294(R)**

Drift-Alfvén Kinetic Stability Theory in the Ballooning Mode Approximation

Bong-Guen Hong and *Duk-In Choi*
Department of Physics
Korea Advanced Institute of Science and Technology
P.O. Box 150
Cheongryangni, Seoul, KOREA

and

W. Horton and *J.E. Sedlak*
Institute for Fusion Studies
The University of Texas at Austin
Austin, Texas 78712

April 1988

Drift-Alfvén Kinetic Stability Theory in the Ballooning Mode Approximation

Bong-Guen Hong and W. Horton
Department of Physics and Institute for Fusion Studies
The University of Texas at Austin
Austin, Texas 78712
and
Duk-In Choi
Department of Physics
Korea Advanced Institute of Science and Technology
P.O. Box 150
Cheongryangni, Seoul, KOREA

Abstract

The coupled drift-shear Alfvén mode including the complete Bessel function gyroradius effect and the $\nabla_\perp B$-curvature guiding center drift resonance of kinetic theory is solved for the toroidal ballooning mode eigenvalues and eigenfunctions. Comparisons between nonlocal (ballooning) and local kinetic theory and between nonlocal fluid and kinetic theory are made. The critical plasma pressure for kinetic ballooning mode instability is only the same as the magnetohydrodynamic (MHD) theory critical pressure $\beta_{\rm MHD}$ for $\eta_i = 0$. The critical kinetic theory plasma pressure $\beta_K(\eta_i)$ is well below $\beta_{\rm MHD}$ and the kinetic theory growth rate is unstable for all k. The MHD second stability region is also unstable in the kinetic theory. The kinetic theory growth rate is a maximum around $k \leq 0.3 - 0.5$ for finite aspect ratio $\varepsilon_n = r_n/R$. The effects of trapped electrons are found to be weakly stabilizing both analytically and numerically, and the instability is still significant outside the ideal MHD stable window from the ion magnetic drift resonances when $\eta_i \gtrsim 1$. The kinetic growth rate is a function of the six dimensionless parameters $k, q^2\beta$, ε_n, s, η_i, and $\tau = T_e/T_i$.

I. Introduction

For finite beta, high temperature plasmas in tokamak confinement systems an accurate description of the drift modes requires kinetic theory. The unstable wavenumber $\mathbf{k}_\perp$ and frequencies $\omega_\mathbf{k}$ are such as to require the full Bessel function description of the ion gyromotion and the Landau resonance of the $\nabla_\perp B$-curvature guiding center drift motion with the wave frequency. The spatially local theory for the full electromagnetic kinetic dispersion relation is given in Horton *et al.*[1] using an algorithm given by Similon *et al.*[2] to compute the kinetic theory response functions called guiding center dispersion functions.

The eigenmodes $\omega_\mathbf{k}$, $\gamma_\mathbf{k}$ of the local 3×3 electromagnetic kinetic theory matrix are shown to have important differences from the corresponding modes described with hydrodynamic theory.[3] Detailed comparisons in the dependence of γ_k on β/β_c, ε_n and η_i are given[1] between the kinetic and hydrodynamic descriptions. Here β_c is defined as the local ideal magneto-hydrodynamic (MHD) pressure limit $\beta = 8\pi(p_i + p_e)/B^2 \leq \beta_c$ for MHD stability [Eq. (62) of Ref. 1], $\varepsilon_n \equiv r_n/R$ (r_n density gradient scale radius and R toroidal major radius), and $\eta_i = d\ell nT_i(r)/d\ell nn_i(r)$. The question addressed in the present work is the change in the stability boundary and growth rate function with respect to the change from local modes to toroidal eigenmodes calculated in the ballooning mode approximations.

The present work is related to the work of Cheng,[4] Tang *et al.*,[5] Andersson and Weiland,[6] and Dominguez and Moore.[7] The present work extends these works by using a more precise description of the ion kinetic response function valid for all ω/ω_{Di} and $k_\perp\rho_i$ and giving a systematic study of the dependence of the growth rate on the five dimensionless parameters $k, q^2\beta, \varepsilon_n, s$ and η_i. The work of Cheng[4] used the full kinetic equation, *but* emphasized the stabilizing effects of the trapped electrons leading him to conclude that for a typical tokamak aspect ratio, the critical beta can be improved by 40%.

The work of Tang *et al.*[5] uses the Rewoldt code[8] which includes electron and ion col-

lisional dissipation and the effects of ion transit and bounce frequency resonant effects. In the Tang *et al.*[5] work, because of the complexity of the modal equations, a rather restricted parametric variation is presented compared with that given in the present work. From studies of the growth rate for PDX,[9] Doublet III[10] and ISX-B,[11] Tang *et al.*[5] conclude that the beta limit of ideal MHD must be viewed as a soft threshold condition with the plasma unstable below the ideal critical beta of MHD. Using an improved two fluid theory, Andersson and Weiland[6] showed that a necessary and sufficient condition for an instability of the MHD branch below the MHD beta limit is the presence of an ion temperature gradient exceeding a threshold. We simplify the problem using the standard circular flux surface model of toroidal equilibrium in contrast to the Dominguez and Moore[7] study using the Ψ, χ flux coordinates of the self-consistent MHD equilibrium. Their study emphasizes the comparisons between two component fluid theory and MHD theory with their kinetic theory restricted to the small $k_\perp \rho_i$ limit. The independent stability parameters are taken from the Ψ variation of typical Doublet III equilibria.

The studies presented here show how the ideal ion kinetic theory plasma gives rise to instability below the MHD stability threshold, and instability in the region of second stability due to the presence of η_i. We also show analytically and numerically that the effects of trapped electrons are weakly stabilizing,[4] and when $\eta_i \gtrsim 1$, the instability is still significant outside of the ideal MHD stable window due to the ion magnetic drift resonances. The variation of the kinetic theory growth rate with parameters also is significantly different from the hydrodynamic growth rate. In particular, the kinetic growth rate is not a monotonically decreasing function of k as in ideal finite Larmor radius (FLR)-MHD theory. In the dynamics described here the electron drift wave is a stable oscillation near ω_{*e}.

In the local electromagnetic dispersion relation there are five branches of oscillation at a given $\mathbf{k}$ which when well separated in frequency are given by $\pm k_\| v_A$, $\pm k_\| c_s$ and ω_{*e} or ω_{*i}, shown, for example, in Fig. 1 of Ref. 3. As the plasma parameters vary the drift modes couple

to the ion-acoustic modes when $k_{||}$ is large ($k_{||}c_s \sim \omega_*$) and to the shear Alfvén wave when $k_{||}$ is small ($k_{||}v_A \sim \omega_*$). Here we assume that $\beta_e = 2c_s^2/v_A^2 \ll 1$. The variation of $k_{||}$ is produced by the connection length qR of the magnetic field line and the shear $s = rq'/q = d\ell nq/d\ell nr$ of the magnetic field. In early studies[12–14] the coupling of the drift modes to the ion-acoustic modes is examined extensively in the ballooning mode approximation. We restrict the present stability study to modes with $\gamma > v_i/qR$ so as to neglect the ion transit time and ion acoustic wave effects. The effects of the ion acoustic coupling are reported elsewhere.[15]

The shear Alfvén wave-electron drift wave coupling problem[16,17] is already difficult in the kinetic theory. The present kinetic drift-shear Alfvén mode theory is difficult because of the interaction of the $v_\perp$ dependence of the ion response with the extended poloidal ballooning mode coordinate ϑ defined over $[-\infty, +\infty]$. Even for small $k = k_\vartheta \rho_s$ the perpendicular wavenumber $k_\perp \rho_s = k(1 + s^2\vartheta^2)^{1/2}$ increases to large values in the toroidal mode eigenfunction. In addition, the large $k_x \rho_s = ks\vartheta$ variation of the wavefunction couples to the geodesic curvature to yield a large drift frequency $|\omega_D(\vartheta)| \gg \omega_k$ for $s\varepsilon_n|\vartheta| \gg 1$. Thus, the kinetic ion response function $P(k, \omega, \vartheta) = \langle(\omega - \omega_{*i})J_0^2(k_\perp v_\perp/\omega_c)/(\omega - \omega_{Di})\rangle_{M-B}$ differs drastically from either the small $|\omega_D/\omega|$ limit or the small $|k_\perp v_\perp/\omega_c|$ limit unless the wavefunction is strongly localized. For typical parameters the eigenfunctions extend to $|\vartheta| \gg \pi$ and the resulting kinetic regime contributions from enhanced ω_D/ω and $k_\perp \rho$ values appreciably lower the critical pressure limit from the local value β_c given in Ref. 1 (Eq. (62)). Above β_c the growth rate γ_k function is similar to that given by local kinetic theory with a broad maximum in k (Ref. 1, Figs. 5,6,8). The $P(k, \omega, \vartheta)$ function is called Q in Dominguez and Moore[7] where it is expanded in small $k_\perp \rho_i$ including terms of order $(k_\perp \rho_i)^4$.

In Sec. II the basic kinetic theory ballooning mode equation is given along with approximate analytic solutions given in two regimes. In Sec. III the results of the eigenvalue stability analysis are given and compared with a simpler nonlocal, hydrodynamic theory and local kinetic theory. We discuss the effects of η_i and trapped electrons on the eigenmodes and

the stability boundary. In Sec. IV we give the conclusions. In the Appendix, we derive the eigenmode equation with trapped electrons.

II. Drift-Shear Alfvén Ballooning Mode Equation

In this work we follow the results and notation of Ref. 1 where possible. The results of Ref. 1 indicate that for β/β_c of order unity the effect of $\delta B_{||}$ is weak. Here we simplify the representation of $\mathbf{E}e^{-i\omega t}$ and $\delta\mathbf{B}e^{-i\omega t}$ to

$$\mathbf{E} = -\nabla\phi + \hat{\mathbf{b}}\hat{\mathbf{b}}\cdot\nabla\psi \qquad \delta\mathbf{B} = \frac{c}{i\omega}\nabla(\hat{\mathbf{b}}\cdot\nabla\psi)\times\hat{\mathbf{b}}. \tag{1}$$

where $i\omega A_{||}/c = \hat{\mathbf{b}}\cdot\nabla\psi$. Following the calculations of the currents and charge densities in Refs. 1-3 we obtain from the condition of quasi-neutrality

$$\hat{a}\phi + \hat{b}\psi = 0 \tag{2}$$

and the parallel component of Ampere's law

$$\hat{b}\phi + \hat{d}\psi = 0 \tag{3}$$

where

$$\hat{a}(k,\omega,\vartheta) = -1 + \tau(P-1) - \frac{c_s^2}{\omega^2 q^2 R^2}\frac{\partial}{\partial\vartheta}P_3\frac{\partial}{\partial\vartheta}$$

$$\hat{b}(k,\omega,\vartheta) = 1 - \frac{\omega_{*e}}{\omega} + \frac{c_s^2}{\omega^2 q^2 R^2}\frac{\partial}{\partial\vartheta}P_2\frac{\partial}{\partial\vartheta}$$

and

$$\hat{d}(k,\omega,\vartheta) = \frac{\rho^2 v_A^2}{\omega^2 q^2 R^2}\frac{\partial}{\partial\vartheta}\nabla_\perp^2\frac{\partial}{\partial\vartheta} - \left(1 - \frac{\omega_{*e}}{\omega}\right)$$
$$+ \left(1 - \frac{\omega_{*pe}}{\omega}\right)\frac{\omega_{De}}{\omega} - \frac{c_s^2}{\omega^2 q^2 R^2}\frac{\partial}{\partial\vartheta}P_1\frac{\partial}{\partial\vartheta}.$$

The relevant frequencies are assumed to be between the transit frequencies of the ions and electrons. The ion kinetic response functions P_j are given by

$$P = \int d\mathrm{v} F_i(\mathrm{v}) \left(\frac{\omega - \omega_{*i}^T}{\omega - \omega_{Di}}\right) J_0^2 \left(\frac{k_\perp v_\perp}{\omega_{ci}}\right) \tag{4}$$

$$P_j = \int d\mathrm{v} F_i(\mathrm{v}) \frac{\omega^{j-1}(\omega - \omega_{*i}^T)}{(\omega - \omega_{Di})^j} \frac{m_i v_\parallel^2}{T_i} J_0^2 \left(\frac{k_\perp v_\perp}{\omega_{ci}}\right)$$

where $F_i(\mathrm{v}) = (2\pi v_i^2)^{-3/2} \exp(-v^2/2v_i^2)$ with $v_i = (T_i/m_i)^{1/2}$ and $\omega_{*i}^T = \omega_{*i}[1 + \eta_i(v^2/v_i^2 - 3/2)]$. The eigenmode equation with trapped electrons is derived in the Appendix.

After neglecting the ion acoustic coupling as discussed in Sec. I, Eq. (2) reduces to

$$A\phi = B\psi \tag{5}$$

and by adding Eqs. (2) and (3) we obtain

$$\widehat{D}\psi = C\phi \tag{6}$$

where

$$\begin{aligned} A(k,\omega,\vartheta) &= -1 - \tau + \tau P(k,\omega,\vartheta) \\ B(k,\omega) &= -1 + \frac{\omega_{*e}}{\omega} \\ C(k,\omega,\vartheta) &= \tau\,[P(k,\omega,\vartheta) - 1] - \frac{\omega_{*e}}{\omega} \\ \widehat{D}(k,\omega,\vartheta) &= \frac{\rho^2 v_A^2}{\omega^2 q^2 R^2} \frac{\partial}{\partial\vartheta} k_\perp^2 \frac{\partial}{\partial\vartheta} - \left(1 - \frac{\omega_{*pe}}{\omega}\right) \frac{\omega_{De}}{\omega}. \end{aligned} \tag{7}$$

Substituting Eq. (5) into Eq. (6) leads to the ballooning mode equation

$$\omega_A^2 \frac{d}{d\vartheta}\left[k_\perp^2(\vartheta) \frac{d\psi(\vartheta)}{d\vartheta}\right] + Q(k,\omega,\vartheta)\psi(\vartheta) = 0 \tag{8}$$

where

$$Q(k,\omega,\vartheta) = (\omega - \omega_{*e})\left[\omega - \omega_{De}(\vartheta) - \frac{\omega - \omega_{*e}}{1 + \tau - \tau P(\vartheta)}\right] \tag{9}$$

and

$$\omega_A^2 = v_A^2/q^2R^2.$$

The ϑ dependence of the functions in Eq. (7) is calculated in the ballooning mode approximation[4,5] where we assumed the circular concentric magnetic flux surfaces,

$$\begin{aligned} k_\perp^2(\vartheta) &= k_\vartheta^2(1+s^2\vartheta^2) \\ \omega_{De}(\vartheta,s) &= 2\varepsilon_n\omega_{*e}(\cos\vartheta + s\vartheta\sin\vartheta) \\ \omega_{Di}(v_\perp^2, v_\parallel^2) &= -\omega_{De}(\vartheta,s)\left(\frac{1}{2}v_\perp^2 + v_\parallel^2\right)\Big/2c_s^2. \end{aligned} \tag{10}$$

If non-uniform shear model is used ($s-\alpha$ model),

$$\begin{aligned} k_\perp^2(\vartheta) &= k_\vartheta^2\left[1+(s\vartheta-\alpha\sin\vartheta)^2\right] \\ \omega_{De}(\vartheta,s) &= 2\varepsilon_n\omega_{*e}\left[\cos\vartheta + (s\vartheta-\alpha\sin\vartheta)\sin\vartheta\right] \end{aligned} \tag{11}$$

and

$$\alpha = \frac{2\varepsilon_n\left[1+\eta_e+(1+\eta_i/\tau)\right]}{\omega_A^2}.$$

In the text of this work we used Eq. (10) for simplicity unless otherwise specified.

To derive the analytic approximations to the eigenvalues we consider the hydrodynamic limit of the ion kinetic integral $P(k,\omega,\vartheta)$. Taking ω_{Di}/ω and $k_\perp\rho_i$ as small parameters in Eq. (4) we obtain the asymptotic expansion

$$P \simeq \alpha_{oi} + \alpha_{1i}\left(\frac{\omega_{Di}}{\omega} - b\right) + \alpha_{2i}\left(\frac{3}{4}b^2 - \frac{3}{2}\frac{b\omega_{Di}}{\omega} + \frac{7}{4}\frac{\omega_{Di}^2}{\omega^2}\right) \tag{12}$$

where $\alpha_{ni} = 1-(\omega_{*i}/\omega)(1+n\eta_i)$ and $b = k_\perp^2\rho_i^2$. Neglecting the second order terms b^2, $b\omega_{Di}/\omega$ and ω_{Di}^2/ω^2 and using the local approximation Eqs. (5) and (6) reduce to Eq. (35) of Ref. 3. The principal ballooning mode equation of Dominguez and Moore[7] [their Eq. (14)] is obtained by neglecting b^2 and $b\omega_{Di}/\omega$ in Eq. (12). Further expansion of the denominator

of the potential Q leads to equations of Tang, *et al.*[18] [their Eq. (3.40)] and Hastie and Hasketh[19] (their Eq. (2.6)).

All frequencies are measured in units of c_s/r_n and the wavenumber k_ϑ in units of $\rho_s = c(m_i T_e)^{1/2}/eB$. The dimensionless frequencies are then given by

$$\omega_{*e} = k \qquad \omega_{*i} = -\frac{k}{\tau} \quad \omega_{De} = 2\varepsilon_n k(\cos\vartheta + s\vartheta\sin\vartheta)$$

$$\omega_A = \left(\frac{2}{\beta_e}\right)^{1/2}\frac{\varepsilon_n}{q} \quad \omega_s = \frac{\varepsilon_n}{q}$$

$\varepsilon_n = r_n/R$ and $\tau = T_e/T_i$. The dimensionless complex frequency $\omega\,[c_s/r_n]$ is a function of the six dimensionless parameters k, $\beta_e q^2$, ε_n, s, η_i and $\tau = T_e/T_i$.

The kinetic eigenvalue problem is given by Eqs. (8)–(9) with the boundary condition that $\psi(\vartheta) \to 0$ as $|\vartheta| \to \infty$ sufficiently rapidly for $\int_{-\infty}^{+\infty} |\psi|^2 d\vartheta < \infty$. In demanding finite $\int_{-\infty}^{+\infty} |\psi|^2 d\vartheta$ we rule out the modes highly localized to the rational surface associated with the Mercier criterion. Localized Mercier modes have $\psi(\vartheta) \to M + N/\vartheta$ and thus $\langle k_x^2\rangle = k^2 s^2 \langle\vartheta^2\rangle \to \infty$. We would not expect such localized modes to be associated with drift wave like anomalous transport since the linear value of $\gamma_k/\langle k_x^2\rangle$ is negligible. The finite square integrable condition on $\psi(|\vartheta| \to \infty)$ also ensures that the kinetic energy of the mode is finite.

The shear Alfvén drift mode wave functions extend into regions of large $k_\perp = k(1 + s^2\vartheta^2)^{1/2}$ where the local ion density fluctuation becomes adiabatic $\tilde{n}_i = -ne\phi/T_i$ since $|P(k_\perp \gg 1)| \ll 1$. This adiabatic ion response gives a lower hybrid electromagnetic drift wave-like contribution to the dispersion relation. Since the bulk of $|\psi(\vartheta)|^2$ is typically in the region $|\vartheta| \lesssim \pi$ the adiabatic ion contribution is subdominant compared with the hydrodynamic ion response. In the region of small $k_\perp^2 = k^2(1+s^2\vartheta^2)$ and $\omega \neq \omega_{*e}$ the parallel electric field is small; however, the parallel electric field is of order unity in the region of small $|P|$.

A. Analytic Ballooning Modes

Here we give approximate analytic formulas that explain several features of the numerical results. The analytic results are obtained from the fluid limit of Eq. (9). Using Eq. (12), Eq. (8) reduces to

$$k^2\omega_A^2\frac{d}{d\vartheta}(1+s^2\vartheta^2)\frac{d}{d\vartheta}\psi+Q\psi=0 \tag{13}$$

where

$$Q(k,\omega,\vartheta)=\omega_{De}[\omega_{*e}-\omega_{*i}(1+\eta_i)]+\alpha_{1i}\omega^2k^2(1+s^2\vartheta^2)-\omega_{De}^2\left(\frac{\alpha_{1i}^2}{1-\frac{\omega_{*e}}{\omega}}+\frac{7\alpha_{2i}}{4\tau}\right).$$

In the limit of $\omega_*/\omega\to 0$, Eq. (13) reduces to the ideal MHD equation, $Q_{\rm mhd}=\omega_{De}[\omega_{*e}-\omega_{*i}(1+\eta_i)]+\omega^2k^2(1+s^2\vartheta^2)-\omega_{De}^2\left(1+\frac{7}{4\tau}\right)$ which is valid for $\omega>\omega_s$ and $k\ll 1$. The terms proportional to ω_{De}^2 arise from the plasma compressibility and the FLR heat flux in fluid equations, and provide additional stability compared with the low-frequency regime (valid for $\omega<\omega_s$). We study Eq. (13) with the finite ε_n, ω_{*i} and the ion temperature gradient effects.

With $s\vartheta=z$ and $\psi(\vartheta)=(1+z^2)^{-1/2}\bar{\psi}(z)$, Eq. (13) transforms to

$$\bar{\psi}''+\left[\frac{Q(z)}{k^2\widehat{\omega}_A^2(1+z^2)}-\frac{1}{(1+z^2)^2}\right]\bar{\psi}=0, \tag{14}$$

where

$$\begin{aligned}Q(z)\;=\;&k^2\Bigg[2\varepsilon_n\left(1+\frac{1+\eta_i}{\tau}\right)(\cos(z/s)+z\sin(z/s))\\&+\left(\left(\omega+\frac{1+\eta_i}{\tau}k\right)(1+z^2)\omega-\left(\frac{\alpha_{1i}^2}{\alpha_{oe}}+\frac{7\alpha_{2i}}{4\tau}\right)4\varepsilon_n^2\left\{\cos(z/s)+z\sin(z/s)\right\}^2\right)\Bigg]\end{aligned}$$

and we put $\widehat{\omega}_A^2=\omega_A^2s^2$. Equation (14) is useful when s is not too small.

We first consider the ideal MHD equation in low-frequency regime ($\omega<\omega_s$).[18] At marginal stability the MHD eigenvalue depends on the combination of β_eq^2, ε_n and τ given by

$$\alpha\equiv\frac{2\varepsilon_n(1+1/\tau)}{\omega_A^2}\equiv\frac{\beta_e(1+1/\tau)q^2}{\varepsilon_n}.$$

The eigenvalue Eq. (14) reduces to

$$\bar{\psi}_0'' + \left[\frac{\alpha\left[\cos(z/s) + z\sin(z/s)\right]}{1+z^2} - \frac{1}{(1+z^2)^2}\right]\bar{\psi}_0 \;=\; 0. \tag{15}$$

If $s-\alpha$ model is employed,

$$\bar{\psi}_0'' - \left[\frac{\left[s - \alpha\cos(z/s)\right]^2}{f^4} - \frac{\alpha\cos(z/s)}{f^2}\right]\bar{\psi}_0 = 0, \tag{16}$$

where

$$f^2 = 1 + \left(z - \alpha\sin\frac{z}{s}\right)^2 \quad \text{and} \quad \bar{\psi}_0 = f\psi_0.$$

The solutions of Eq. (16) for $\alpha = \alpha(s)$ are the well known MHD ballooning beta limits and given[20] as $\alpha_1 \cong s^{1/2}$ and $\alpha_2 \cong 2.5s^{1/2}$ for $s \sim \alpha^2 < 1$ and $\alpha_{1,2} \simeq c_{1,2}s$ for $s \sim \alpha \gtrsim 1$.

We approximate the effective potential

$$V_{\text{eff}}(z) = \frac{1}{(1+z^2)^2} - \frac{Q(z)}{k^2\widehat{\omega}_A^2(1+z^2)}$$

as a well which has a local minimum at $z = z_0$, i.e.,

$$V_{\text{eff}}(z) \cong V_{\text{eff}}(z_0) + \frac{(z-z_0)^2}{2}\frac{d^2}{dz^2}V_{\text{eff}}(z)\bigg|_{z=z_0},$$

then Eq. (14) becomes

$$\bar{\psi}'' - \left[V_{\text{eff}}(z_0) + \frac{1}{2}V_{\text{eff}}^{(2)}(z_0)(z-z_0)^2\right]\bar{\psi} = 0. \tag{17}$$

Solution of Eq. (17) is $\psi_n(\xi) \sim H_n\exp(-\xi^2/2)$ and eigenvalue condition is

$$V_{\text{eff}}(z_0) = -\left[\frac{1}{2}V_{\text{eff}}^{(2)}(z_0)\right]^{\frac{1}{2}}(2n+1) \tag{18}$$

where z_0 is a solution of $dV_{\text{eff}}(z_0)/dz = 0$.

Using Eq. (14), we obtain

$$-V_{\text{eff}}(z_0) \;=\; \frac{Q(z_0)}{k^2\widehat{\omega}_A^2(1+z_0^2)} - \frac{1}{(1+z_0^2)^2}$$

and

$$V_{\rm eff}^{(2)}(z_0) \;=\; \frac{2Q(z_0)-Q''(z_0)(1+z_0^2)}{k^2\widehat{\omega}_A^2(1+z_0^2)^2} - \frac{4(1-z_0^2)}{(1+z_0^2)^4}.$$

The width of the mode is given by

$$s\Delta\vartheta = \Delta z = \left(V_{\rm eff}^{(2)}(z_0)\right)^{-1/4}$$

and we require $\left|k_{||}c_s/\omega\right| = \varepsilon_n/(q|\omega|\Delta\vartheta) < 1$ for consistency.

We divide the parameter space with the two regimes by $\widehat{\omega}_A^2 < 0.2$ and $\widehat{\omega}_A^2 > 0.2$.

In the first regime $\widehat{\omega}_A^2 < 0.2$, the minimum is at $z_0 \sim 0$ and the condition of Re $\left[V_{\rm eff}^{(2)}(0)\right] > 0$ gives $\varepsilon_n < 0.2$, so that ω_{De}^2 terms are not important. Neglecting the right-hand side of Eq. (18), we obtain from $V_{\rm eff}(0) = 0$, the eigenvalue as

$$\omega_r^{(0)} \;=\; -(1+\eta_i)k/2\tau \tag{19}$$

and

$$\gamma_k^{(0)} \;=\; \left[2\varepsilon_n\left(1+\frac{1+\eta_i}{\tau}\right) - \widehat{\omega}_A^2 - \frac{(1+\eta_i)^2k^2}{4\tau^2}\right]^{1/2}. \tag{20}$$

The growth rate $\gamma_k^{(0)}$ is the same as given by local theory with $k_{||} = s/qR$ and $\vartheta = 0$. Eq. (20) shows that the finite Larmor radius effects are stabilizing. Following our earlier local theory analysis we define the local MHD critical beta $\beta_{\rm c}$ below which the hydrodynamic growth rate vanishes in the $k \to 0$ limit. Including the temperature gradient parameters the general result (Eq. (43) of Ref. 3) is

$$\beta_{\rm c}^{\rm MHD} = \frac{\varepsilon_n(1+1/\tau)}{q^2[1+\eta_e+\frac{1+\eta_i}{\tau}]} \quad \text{or} \quad \alpha = \frac{2\varepsilon_n\left(1+\eta_e+\frac{1+\eta_i}{\tau}\right)}{\omega_A^2} = \beta/\beta_{\rm c}^{\rm MHD}.$$

In the present work we consider only $\eta_e = 0$ for simplicity. Solution (19)–(20) shows that the growth rate increases as $\sqrt{\varepsilon_n}$ for given values of β and s and that increasing shear weakly reduces the growth rate for given values of β and ε_n. Equation (20) also shows that to have an unstable root ε_n should have a small but finite value.

In the second case of $\widehat{\omega}_A^2 > 0.2$, the minimum of $V_{\rm eff}(z)$ occurs at $z_0 \sim \pi s/2$ where ε_n, s have larger values compared with the first case, so that the ω_{De}^2 terms cannot be neglected. For these parameter values, the condition $\mathrm{Re}\left[V_{\rm eff}^{(2)}(z_0)\right] > 0$ is well satisfied up to $\varepsilon_n \sim 0.5$. We solve the eigenvalue equation by treating the ω_{De}^2 terms as a perturbation. With $\omega = \omega^{(0)} + \Delta\omega$ and from $V_{\rm eff}(z_0) = 0$, we obtain

$$\omega_r^{(0)} = -\frac{(1+\eta_i)k}{2\tau}$$

$$\gamma_k^{(0)} = \left[\frac{2_n\left(1+\frac{1+\eta_i}{\tau}\right)\frac{\pi}{2}s - \frac{\widehat{\omega}_A^2}{1+\frac{\pi^2}{4}s^2}}{1+\frac{\pi^2}{4}s^2} - \frac{(1+\eta_i)^2k^2}{4\tau^2}\right]^{1/2} \tag{21}$$

and

$$\Delta\omega = \frac{\varepsilon_n^2\pi^2 s^2}{2\left(1+\frac{\pi^2 s^2}{4}\right)}\frac{1}{\omega_0^2}\left[\frac{\left(\omega_0+\frac{1+\eta_i}{\tau}k\right)^2}{\omega_0-k} + \frac{7}{4\tau}\left(\omega_0+\frac{1+2\eta_i}{\tau}k\right)\right].$$

The sign of $\Delta\omega$ is negative when $|\omega_{*pi}/\omega| < 1$ and gives a stabilizing effect: when $|\omega_{*pi}/\omega| > 1$, the ω_{De}^2 terms change sign from stabilizing to destabilizing. In this regime $\widehat{\omega}_A^2 > 0.2$ or $\beta \lesssim 10\varepsilon_n^2/q^2$ the geodesic component of the toroidal curvature is the dominant driving mechanism. The line bending stabilization from $\widehat{\omega}_A^2$ is reduced to $\widehat{\omega}_A^2 \to \widehat{\omega}_A^2/(1+\pi^2 s^2/4)$ by the broader spread $\Delta\vartheta$ of the wave function. When $|\omega_{*pi}/\omega| < 1$, Eq. (21) shows that there is an upper boundary for ε_n, above which the plasma is stable. The critical ε_n for stability is a function of s. For $s \sim 1$, the upper boundary for ε_n is 0.25, and for $s \sim 0.5$ it is 0.3. From this we can see that the role of shear is stabilizing by making the stabilizing perpendicular compression of the plasma dominant over the interchange energy release in the parameter range $\varepsilon_n \geq \epsilon_n(s)$.

B. Numerical Analysis of the Ballooning Modes

The ballooning mode Eqs. (8)–(9) and Eq. (A13) in the Appendix with trapped electrons are solved numerically using the standard shooting method. The boundary condition is that the wave function vanish sufficiently rapidly as $|\vartheta| \to \infty$ so that $\int_{-\infty}^{+\infty} |\psi|^2 d\vartheta < \infty$. In solving

the complete eigenmode equation given in Eq. (A13), we take into account the energy and the velocity space pitch angle dependence of the bounce averaged electron drift frequency

$$\bar{\omega}_{De} = \frac{\int_{-\vartheta_0}^{\vartheta_0} \frac{d\vartheta}{|v_{||}|} \omega_{De}}{\int_{-\vartheta_0}^{\vartheta_0} \frac{d\theta}{|v_{||}|}},$$

where $-\vartheta_0$ and ϑ_0 are the nearest turning points. The details of the derivations are given in the Appendix.

III. Stability Properties

First we show the spectrum of unstable oscillations as a function of $k_\vartheta \rho_s = k$ for typical MHD unstable tokamak parameters in Fig. 1. We choose $\varepsilon_n = .25$, $s = 1$, $q = 2, \tau = 1$, $\alpha = \beta/\beta_c = 1.0$ and 2.0 where $\beta_c = \varepsilon_n/q^2 = 0.0625$ which are the same parameters used in Ref. 1 (note $\eta_i = \eta_e = 0$ only in Fig. 5b of Ref. 1). For direct comparison we repeat here the local kinetic theory growth rate computed with $k_{||} = 1/qR$ ($= s/qR$ for $s = 1$) for the $\beta/\beta_c = 2.0$ case given by the dashed line.

Considering the $\beta/\beta_c = 2$ mode in Fig. 1 we observe that the frequency is almost dispersionless with a speed $\omega/k \cong -0.3[c_s\rho_s/r_n]$ in the ion diamagnetic direction. Thus, the mode resonates $\omega_k = \omega_{Di}(v^2)$ with ions near one-half the thermal energy since $E_r/T_i = -\omega/2k\varepsilon_n = 0.6$. Only for $\varepsilon_n \to 0$ is the resonance restricted to the high energy ions. The growth rate increases linearly for $k \lesssim 0.25$ and has a broad maximum at $k \simeq 0.5$.

In Fig. 2 we show the $\eta_i = 2$ spectrum of oscillations for $\alpha = \beta/\beta_c = 1$ and 2, which is to be compared with the $\eta_i = 0$ spectrum in Fig. 1. At $\beta = \beta_c$ the maximum growth rate increases by a factor of 3 in going from $\eta_i = 0$ to $\eta_i = 2$, but at small k the growth rate still vanishes linearly with k. For $\beta = 2\beta_c$ and $\eta_i = 2$ the growth rate finally shows the FLR-MHD behavior of $\gamma(k \to 0) \to \gamma_o = \text{const}$. This same condition that $\eta_i > \eta_i^{\text{crit}}$ (of order one) be satisfied before the $k \to 0$ growth rate approaches a constant was found in

local kinetic theory Ref. 1, Fig. 5.

Now we fix the wavenumber k in the region of maximum growth rate and vary the plasma pressure. In Fig. 3(a) we give the growth rate from ballooning kinetic theory Eq. (8) and the ideal MHD ballooning mode Eq. (15). The kinetic threshold beta is given by $\beta_K = 0.0374$ or $\alpha_c = 0.6$. Thus, the ballooning mode has a substantially lower threshold than the local approximation due to the destabilizing geodesic component of the toroidal drift frequency $\omega_D(\vartheta)$. In Fig. 3(b) we did the same calculation with so-called "$s-\alpha$ model".[21] The second stability region appears for large $\alpha_c \simeq 2.65$ values. The stabilizing effect of trapped electrons is also shown by solving Eq. (A13) derived in the Appendix with the pitch angle dependence correctly treating. The relative shift in α_c is 33% for the first stability boundary and 14% for the second stability boundary.

For analytic analysis of the effects of trapped electrons, we use $G_1(\kappa)+sG_2(\kappa) \sim 0.5$, for $\bar{\omega}_{De}$ in Eq. (A5) which is a good approximation for $s \sim 1$ or deeply trapped particles, and use a fluid expansion, then we obtain

$$\frac{\omega_A^2}{\omega^2}\frac{d}{d\vartheta}\nabla_\perp^2\frac{d}{d\vartheta}\psi + \left\{\frac{\omega_{De}(\omega_{*pi}-\omega_{*pe})}{\omega^2} - k_\perp^2\left(1-\frac{\omega_{*pi}}{\omega}\right) + \frac{\omega_{De}^2}{\omega^2}\left(\frac{7}{4\tau}\alpha_{2i} + \frac{\alpha_{1i}\alpha_{1e}}{\alpha_{0e}}\right)\right.$$

$$\left. + \sqrt{2\varepsilon_0}\,\frac{\omega_{De}^2}{4\omega^2}\left[\frac{\alpha_{1e}}{\alpha_{0e}}(\alpha_{1i}-3\alpha_{1e}) + \frac{15}{4}\alpha_{2e}\right]\right\}\psi = 0. \tag{22}$$

The last term of Eq. (22) is from the trapped electron effects and it is relatively weak; i.e., of order $\mathcal{O}\left(\sqrt{2\varepsilon_0}\,\frac{\omega_{De}^2}{\omega^2}\right)$. It is interesting to note that, up to order $\mathcal{O}\left(\sqrt{2\varepsilon_0}\,\frac{\omega_{De}}{\omega}\right)$ there is no contribution from the trapped electrons to MHD ballooning mode. Terms of this order arise from both electrostatic and electromagnetic components, but they cancel each other. In the limit of $|\omega_*/\omega| \ll 1$, the effects of trapped electrons are weakly stabilizing. When $|\omega_*/\omega|$ is finite we must solve Eq. (22) to determine the effects of the trapped electrons. But for a more accurate description of the effect of trapped electrons we rely on the numerical solution of Eq. (A13) which does not use the expansion in $|\omega_{De}/\omega|$.

Both the kinetic mode and the MHD mode have the same threshold beta at $\eta_i = 0$ although the rate of increase of the kinetic growth rate above β_K is appreciably slower than the MHD growth rate. To understand why the threshold beta is the same for the kinetic and MHD theory we need to compare the eigenmode equations at the threshold frequency. The kinetic mode marginal frequency is $\omega = \omega_{*i}$ where $\mathrm{Im}(P) = \mathrm{Re}(P) = 0$. The MHD marginal frequency is $\omega^2 = 0$. Reducing Eq. (8) at $\omega = \omega_{*i}$ one readily shows that it is the same equation as the $\omega^2 = 0$ ideal MHD Eq. (15). This conclusion also holds for more general cases, Eqs. (2) and (3), in which $P = 0$ and $P_j = 0$ at $\omega = \omega_{*i}$. The ion acoustic couplings do not change the marginal stability for $\eta_i = 0$.

For $\eta_i \neq 0$, the kinetic response function does not vanish at the MHD marginal stability frequency. For $\omega \cong \omega_{*i}$, the η_i response adds to the $V_{\mathrm{eff}}(z)$ through the function

$$\Delta P(\omega_{*i}, k, z) = -\eta_i P \left\langle \frac{(v^2/v_i^2 - 3/2) J_0^2(k_\perp v_\perp/\omega_{ci})}{1 - \omega_{Di}(v_\perp, v_{||}, z)/\omega_{*i}} \right\rangle$$

$$+ i\eta_i \sqrt{2\pi}\,\widehat{\omega}_z H(\widehat{\omega}_z) \int_0^{\widehat{\omega}_z^{1/2}} dv_{||} e^{v_{||}^2/2 - \widehat{\omega}_z} J_0^2 \left(k_\perp \sqrt{2(\widehat{\omega}_z - v_{||}^2)}\right)$$

$$\times \left(\frac{3}{2} + \frac{1}{2} v_{||}^2 - \widehat{\omega}_z\right), \tag{23}$$

where $\widehat{\omega}_z = \frac{2\omega_{*i}}{\omega_{Di}(z,s)}$ and H is the heaviside step function. The second term in the right hand side of Eq. (23) is from the ion magnetic resonance contribution. In the neighborhood of small η_i we expand Eq. (8) using the $s - \alpha$ model about the MHD marginal stability frequency with $\omega = \omega^{(0)} + \Delta\omega^{(1)}$, and we obtain

$$\bar{\psi}'' - \left\{ \frac{(s - \alpha \cos z/s)^2}{f^4} - \frac{\alpha \left[\cos z/s + \frac{(\omega^{(1)}/\omega_{*i})[1 - \Gamma_0(k_\perp)] - \Delta P}{2\epsilon_n(1+\tau)}\right]}{f^2} \right\} \bar{\psi} = 0, \tag{24}$$

where $\bar{\psi} = f\psi$ as defined in Eq. (16).

Perturbation theory for the complex frequency shift $\Delta\omega^{(1)}$ due to η_i gives

$$\Delta\omega^{(1)} = \omega_{*i} \frac{\int_{-\infty}^{\infty} dz \frac{\bar{\psi}_0^2}{f^2} \Delta P}{\int_{-\infty}^{\infty} dz \frac{\bar{\psi}_0^2}{f^2} (1 - \Gamma_0(k_\perp \rho_i))}. \tag{25}$$

Solution of Eq. (16) for marginal stability with $s \sim \alpha \geq 1$ is $\bar{\psi}_0 \sim e^{-\alpha\vartheta^2/4}$ and

$$\Delta P \sim -\eta_i(2\varepsilon_n - k_\perp^2) + i\eta_i \left(\frac{\sqrt{2\pi}}{\sqrt{\varepsilon_n}}\right) e^{-\frac{1}{2\varepsilon_n}} \left(\frac{3}{2} - \frac{1}{2\varepsilon_n}\right).$$

We obtain $\Delta\omega^{(1)}$ as

$$\Delta\omega^{(1)} \sim \omega_{*i} \left(\eta_i - c_1 \frac{2\varepsilon_n \eta_i}{k^2}\right) + i\omega_{*i}\eta_i c_2 \frac{e^{-1/2\varepsilon_n}}{k^2\sqrt{\varepsilon_n}} \left(\frac{3}{2} - \frac{1}{2\varepsilon_n}\right), \tag{26}$$

with $c_1 = 0.1573 \cdot e \cdot \sqrt{\pi}$ and $c_2 = \sqrt{2\pi} c_1$. Equation (26) shows the instability outside the ideal MHD stable windows exist when $\eta_i \neq 0$ and $\varepsilon_n < 1/3$. For $\varepsilon_n > 1/3$ the resonance gives damping of the marginal MHD mode.

For fixed wavenumber $k = 0.5$ and the system parameters used in Fig. 3 except for $\eta_i = 2.0$ we obtain the beta dependence of the growth rate shown in Fig. 4(a). With $\eta_i = 2.0$ the system is unstable for $\beta > \beta_K(\eta_i = 2) \simeq 0.006$ ($\alpha_c = 0.144$) and the growth rate increases to $\gamma_k \cong 0.287$ at the local MHD beta critical $\beta = \beta_c = 0.04$. Thus, we find that $\eta_i = 2.0$ reduces the critical plasma pressure by $\beta_K(\eta_i = 2)/\beta_K(\eta_i = 0) \sim 0.16$. For $\beta \sim \beta_K(\eta_i)$ the growth rate is vanishing by definition of marginal stability and the effects of finite $\omega_{ti} = v_i/qR$ may be important. The marginal mode frequency approaches $\omega_{*pi} = \omega_{*i}(1 + \eta_i)$.

In Fig. 4(b) the growth rate and frequency using $s - \alpha$ model are presented. With $\eta_i = 2$, instability is significant outside of the ideal MHD stable window. The small but finite instability of the MHD second stability region is important in view of transport since the wave functions are localized in θ, implying small $\langle k_x^2 \rangle$. With the inclusion of trapped electrons, the growth rate is still significant outside the MHD stable window due to the thermal ion magnetic resonance effect when $\eta_i \gtrsim 1$. In this case the trapped electrons give relatively weak stabilizing effect compared with the $\eta_i = 0$ case.

Next we study the variation of the growth rate with toroidicity ε_n. For small ε_n the growth rate increases with $\left(\varepsilon - \varepsilon_n^{\rm crit}\right)^{1/2}$ as given by Eq. (20) and shown in Fig. 5. At small ε_n the growth rate is insensitive to the variation in s. As ε_n increases well above the threshold value $\varepsilon_n^{\rm crit}$ the growth rate reaches a maximum value and then slowly decreases for large values of s. The stabilizing effect for larger ε_n arises from the compressional effects and FLR heat flux described by the ω_{De}^2 terms in the fluid expansion in Eq. (13). The analytic approximation for this stabilization is described by formula (21) valid for $\widehat{\omega}_A^2 > 0.2$. Formula (21) predicts stability for $\pi\varepsilon_n s \gtrsim 1$ where the kinetic ballooning shows a strong decrease in the growth rate.

Now we consider the dependence of the growth rate on shear $s = rq'/q$. Both the small and large aspect ratio systems are shown in Fig. 6 at $\beta = 0.09375$. Here the growth rate for $\varepsilon_n = 0.25$ decreases faster than the $\varepsilon_n = 0.1$ growth rate due to the stabilizing ε_n^2 terms in Eq. (21) arising from compressibility. The variation of the growth rate with shear is weak for the small aspect ratio $\varepsilon_n = 0.1$. Both growth rates show a maximum near $s = 0.3$.

Some stability properties of the system can be understood from the constraint imposed by multiplying Eq. (8) by $\psi^*(\vartheta)$ and integrating over ϑ. Evaluating the equation for real ω we obtain the condition for a marginally stable mode

$$\int_{-\infty}^{+\infty} d\vartheta \frac{|\psi(\vartheta)|^2 \, ImP(k,\omega,\vartheta)}{|1+\tau-\tau P(k,\omega,\vartheta)|^2} = 0 \tag{27}$$

and

$$\frac{q^2\beta_e}{2\varepsilon_n^2} = \frac{k^2 \int_{-\infty}^{+\infty} d\vartheta (1+s^2\vartheta^2) \left|\frac{d\psi}{d\vartheta}\right|^2}{(\omega-\omega_{*e}) \int_{-\infty}^{+\infty} d\vartheta \, |\psi(\vartheta)|^2 \left[\omega - \omega_{De} - \frac{(\omega-\omega_{*e})(1+\tau-\tau P_r)}{|1+\tau-\tau P|^2}\right]} \tag{28}$$

where $P_r = ReP(k,\omega,\vartheta)$. Equation (27) determines the marginal frequency ω_m and Eq. (28) gives the critical β_e above which the system is unstable.

The only case for which Eqs. (27)–(28) may be solved analytically is for $\eta_i = 0$ where

$\omega_m = \omega_{*i}$ is the exact marginal stability frequency, and Eq. (28) reduces to

$$\alpha_c = \frac{q^2\beta_e\left(1+\frac{1}{\tau}\right)}{\varepsilon_n} = \frac{\int_{-\infty}^{+\infty} d\vartheta(1+s^2\vartheta^2)\left|\frac{d\psi}{d\vartheta}\right|^2}{\int_{-\infty}^{+\infty} d\vartheta\,|\psi(\vartheta)|^2\,(\cos\vartheta + s\vartheta\sin\vartheta)} \tag{29}$$

where we use $P_r = \mathrm{Re}\,P(\omega_m) = 0$ and $\omega_m - \omega_{De} - (\omega_m - \omega_{*e})/(1+\tau) = -\omega_{De}$ in Eq. (28).

For $\eta_i \neq 0$ we have no exact results from Eqs. (27)–(28). For fixed or local value of ϑ the condition $\mathrm{Im}\,P = 0$ yields the marginal stability frequency

$$\omega_m = \frac{\omega_{*i}(1-\frac{3}{2}\eta_i)}{1-\frac{\eta_i\omega_{*i}}{\omega_{Di}}} \tag{30}$$

and the value of $P_r = ReP(\omega_m) = c_m\eta_i\omega_{*i}/\omega_{Di} \simeq 0.7R/r_{Ti}$ where $\eta_i = r_n/r_{Ti}$ and c_m is a constant. This leads to the instability condition of

$$\varepsilon_{Ti} = \frac{r_{Ti}}{R} < \frac{0.7}{1+\tau} \tag{31}$$

for electrostatic η_i mode. We study the local electromagnetic dispersion relation,

$$D^{\mathrm{EM}} = k^2\omega_A^2 - (\omega-\omega_{*e})\left[\omega - \omega_{De} - \frac{\omega-\omega_{*e}}{1+\tau-\tau P}\right]$$

in three η_i regimes: $\eta_i < 2\varepsilon_n$, $2\varepsilon_n < \eta_i < 2/3$ and $\eta_i > 2/3$ using the Nyquist analysis shown in Fig. 7 for the $\eta_i > \frac{2}{3}$ regime. For $\eta_i < 2\varepsilon_n$, the Nyquist analysis shows the MHD ballooning mode is unstable when $\beta > \varepsilon_n/q^2 = \beta_c^{\mathrm{MHD}}$. For $2\varepsilon_n < \eta_i < 2/3$, $\mathrm{Im}\,P = 0$ has no root and Nyquist analysis gives one unstable root for all beta values, which means that in this range of η_i values the MHD ballooning mode is threshold-free. When $\eta_i > 2/3$, two unstable roots are possible for

$$\beta_e < \frac{\varepsilon_n}{q^2\left(1+\frac{2}{\pi\tau\eta_i}\right)}.$$

In this range of η_i-values, the MHD ballooning branch is unstable for all beta values and the unstable electrostatic η_i branch is stabilized by finite beta effects for $q^2\beta_e > \epsilon_n/(1+2/\pi\tau\eta_i)$. The change of stability properties at $q^2\beta_e \sim \varepsilon_n/[1+(2/\pi\tau\eta_i)]$ for $\eta_i > 2/3$ is shown in Fig. 7. When β_e changes from $\beta_e = 0.01$ (Fig. 7c) to $\beta_e = 0.02$ (Fig. 7d), then $D_r(\omega_m)$ becomes negative and the Nyquist analysis shows one unstable root, the MHD ballooning mode.

A. Marginal Stability

From the shooting code analysis we observe that the wave functions near marginal stability extend to large ϑ so that the integrals in Eqs. (27)–(28) average $P(k,\omega,\vartheta)$ and $\omega_{De}(\vartheta)$ over many oscillations. We find that the results in this regime are sensitive to the decay rate of the asymptotic wave function ($\psi \sim \vartheta^{-\mu}$). In particular, the critical plasma pressure depends on the value of μ. In this subsection we briefly discuss this dependence and argue that the inclusion of additional physics makes the choice of μ.

For large ϑ the ion response function vanishes as $|P(\vartheta)| \sim 1/\vartheta^2$ so that the ion response is adiabatic. In this large ϑ region only the electrons are magnetized and contribute to the bad curvature drive of the instability according to

$$\frac{d}{d\vartheta}\vartheta^2\frac{d\psi}{d\vartheta} + \frac{(\omega-\omega_{*e})}{k^2\omega_A^2 s^2}\left[\omega - \omega_{De}(\vartheta) - \frac{(\omega-\omega_{*e})}{1+\tau}\right]\psi \cong 0 \tag{32}$$

obtained from Eq. (8) for $\vartheta^2 \gg (1+1/k^2)/s^2$ and $\omega_{De}(\vartheta) \simeq 2k\varepsilon_n s\vartheta\sin\vartheta$. The asymptotic wave function $\psi_\infty(\vartheta)$ decays as

$$\psi_\infty(\vartheta) \;=\; A_+\vartheta^{-\mu_+} + A_-\vartheta^{-\mu_-}$$

with

$$\mu_\pm(\omega) \;=\; \frac{1 \pm (1-4D_\omega)^{1/2}}{2}$$

where

$$D_\omega = \frac{(\omega-k)}{k^2\omega_A^2 s^2}\left[\frac{\omega+k/\tau}{1+1/\tau} + (\omega-k)\frac{2\varepsilon_n^2}{\omega_A^2}\right]. \tag{33}$$

In the critical MHD regime $\beta \sim \beta_c$ where $\omega_A^2 \sim 2\varepsilon_n$ the function D_ω reduces to $D_\omega \simeq (\omega-k)(\omega+k/\tau)/(k^2\omega_A^2 s^2(1+1/\tau))$. Thus, in the high frequency regime $|\omega| > k$, D_ω exceeds $1/4$ giving slowly oscillating wave functions at infinity. For the low frequency MHD-like modes near marginal stability $D_\omega \simeq -1/\omega_A^2 s^2(1+\tau)$ and only the branch μ_+ is allowed by the boundary condition at $|\vartheta| \to \infty$.

The kinetic theory result for the asymptotic wave functions is in contrast to the MHD result where $D_{\rm MHD} \simeq 2\varepsilon_n^2[1+(1+\eta_i)/\tau]^2/\omega_A^4$. This is less than 1/4 for small β and the system is stable (Mercier criterion). The different result for D_ω in Eq. (33) arises from the different asymptotic behavior of P in the kinetic and MHD theories. In the MHD model the small k high frequency expansion of P in Eq. (12) is extended to $k_\perp \to \infty$ in the asymptotic analysis. In kinetic theory the $k_\perp \sim ks\vartheta \to \infty$ limit gives $P \to 1/\vartheta^2$ due to the $J_0^2(k_\perp v_\perp/\omega_{ci})$ and the ω_{Di} functions in P in Eq. (4).

Alternatively, we note that for eigenmodes with small growth rates ($\gamma r_n/c_s < .04 \sim .05$) the wave functions extend to $\vartheta_{\rm max} > (m_i/m_e)^{1/2}/ks$. In this regime we modify Eq. (32) to include the effects of the finite electron gyroradius to absorb the outgoing wave energy. The asymptotic wave function decays as $\psi_\infty \sim 1/\vartheta$ without oscillations. We argue that this is the proper physical boundary condition in the case of highly extended wave functions.

Our numerical tests indicate that the Mercier-like boundary condition gives a growth rate that lies everywhere below the MHD growth rate. The critical plasma pressure is found to be very close to the MHD value when Mercier-like boundary conditions are used. However, the inclusion of the kinetic theory energy absorption mechanism at large ϑ leads to the growth rate shown in Fig. 4. Thus, the system remains unstable for beta well below the MHD critical beta in kinetic theory.

IV. Conclusions

Fully kinetic local stability studies for pressure gradient driven modes in a tokamak are reported in Ref. 1 showing the substantial modification of local fluid theory modes. Due to these kinetic theory modifications from the predictions of fluid theory the question arises if the ballooning modes, which require large $k_\perp$ response functions even for a mode with small $k_\vartheta \rho_i$, are given adequately by the hydrodynamic approximation to the ion response functions. The hydrodynamic approximation to the response functions has been used extensively by

Hastie *et al.*,[13,19] Tang *et al.*,[18] Itoh *et al.*,[17] and others.

Here we report the ballooning mode eigenvalues with the full kinetic response function for the ions. We keep both $v_\perp$ and $v_{||}$ integrals in the $\nabla_\perp B$-curvature guiding center response function and the full Bessel function response function.

Our stability analysis shows that there are two regimes for the eigenvalues. In the first regime $\widehat{\omega}_A^2 < 0.2$ or $\beta > 20\varepsilon_n^2 s^2/q^2$ the behavior is similar to magnetohydrodynamic theory in Eq. (20) with the growth rate increasing as $\varepsilon_n^{1/2}$ and decreasing with shear. In the second regime $\widehat{\omega}_A^2 > 0.2$ or $\beta < 20\varepsilon_n^2 s^2/q^2$ the growth rate behaves differently from the classical result due to the importance of shear and the shifted minimum of $V_{\text{eff}}(z)$. As shown in Figs. 5 and 6 and indicated by Eq. (21) the growth rate reaches a maximum for $0.1 < \varepsilon_n < 0.2$ and $0.3 \leq s \leq 0.5$. The maximum growth rate is $\gamma_m \leq 0.6\varepsilon_n^{1/2}(c_s/r_n)$, and is reached for modes with $k_\vartheta \rho \gtrsim 0.3$. At small $k_\vartheta \rho$ the growth rate is smaller and increases $\gamma_k \simeq k_\vartheta \rho\,[2\varepsilon_n(1-\beta_K/\beta)]^{1/2}$ which is very different from FLR-MHD theory where $\gamma(k)$ is monotonically decreasing with increasing k.

For $\eta_i = 0$ we show that the kinetic theory threshold β_K is the same as the MHD threshold beta. This result is clearly shown in Fig. 3 and arises from the fact that at the marginal stability frequency $\omega = \omega_{*i}$ the entire ion kinetic response function $P(k,\omega,\vartheta)$ vanishes identically. Inclusion of the ion acoustic coupling does not change the marginal stability. Eqs. (2) and (3) at $\omega = \omega_{*i}$ reduce to the ideal MHD Eq. (15) with $\omega = 0$. For $\eta_i \neq 0$ there is no frequency for which $P(k,\omega,\vartheta)$ vanishes identically and there is appreciable destabilization from the η_i contribution of $P(k,\omega_{*i},\vartheta)$. The result is that the critical beta value for instability $\beta_K(\eta_i)$ is found to be considerably smaller than the corresponding ideal MHD ballooning mode value. An example for $\eta_i = 2$ is studied in detail.

For the effects of trapped electrons we showed both analytically and numerically that their effect is weakly stabilizing. The trapped electron contribution reduces the growth rate but the kinetic instability instability outside the ideal MHD stable window remains

significant when $\eta_i \gtrsim 1$.

Finally, we note that the simple MHD theorem of a sufficient condition for instability for modes with asymptotic wave functions $\psi(\vartheta) \simeq A/\vartheta^\mu$ having $\mu = 1/2 \pm i(D - 1/4)^{1/2}$ when $D > 1/4$ (Mercier criterion) is lost in the kinetic eigenvalue equation Eqs. (8)–(9) since the instability proof follows from adding the $k_\perp^2(\vartheta)\omega(\omega - \omega_{*i}) < 0$ kinetic energy contribution in the MHD equation (13). In kinetic theory the asymptotic form of the potential $Q(k, \omega, \vartheta)$ is altogether different [Eq. (32)] with the ions giving an adiabatic response $\tilde{n}_i \simeq -n_o(e_i\phi/T_i)$ in contrast to the classical hydrodynamic response in Eq. (12). The asymptotic analysis of the kinetic Eq. (8) yields the critical exponents $\mu_\pm = 1/2 \pm i(D_\omega - 1/4)^{1/2}$ with $D_\omega \cong (\omega - k)(\omega + k/\tau)/k^2\omega_A^2 s^2$. In kinetic theory $D > 1/4$ requires $|\omega| > k$ and $q^2\beta > \varepsilon_n^2 s^2/4$. The oscillatory wave functions for $D > 1/4$ describe the propagation of wave energy to $|\vartheta| \to \infty$ where absorption by microscopic processes such as electron Landau damping occurs. Explicitly including such processes in the boundary condition leads to a kinetic theory instability which increases gradually with beta, obtaining a substantial value at the ideal MHD threshold plasma pressure.

Thus, we conclude that the dynamics of the unstable plasma is considerably different in the kinetic description than in the ideal FLR-MHD theory. The only exception, where the kinetic theory behavior reduces to the fluid theory, is where $\varepsilon_n \ll 0.1$. In this large aspect ratio regime the number of resonant ions is exponentially small and the growth rate follows the FLR-MHD theory.

Acknowledgments

The authors thank Dr. J.E. Sedlak for his work on the eigenvalue problem during the course of this project. The work was supported by the U.S. Department of Energy Contract No. DE-FG05-80ET-53088, and by the Korea Advanced Institute of Science and Technology.

Appendix — Role of the Trapped Electrons

In this Appendix we derive the generalization of eigenmode Eq. (8) that includes the effect of the trapped electrons.

The solution of the gyrokinetic equation f_j is written as

$$f_j = -(e_j/T_j)\phi F_j + g_j \exp(iL_j), \tag{A1}$$

with $L_j = \mathbf{k}\cdot\mathbf{v}\times\widehat{\mathbf{b}}/\Omega_j$ and $\Omega_j = e_jB/m_jc$. The nonadiabatic part g_j satisfies

$$\left(v_{\|}\frac{\partial}{\partial s} - i(\omega-\omega_{Dj})\right) g_j = -iF_j(\omega-\omega_{*tj})\left[\frac{e_j}{T_j}(\phi - v_{\|}A_{\|})J_0\right], \tag{A2}$$

where $i\omega A_{\|} = \widehat{\mathbf{b}}\cdot\nabla\psi$. The frequencies of the modes we are interested in are assumed bounded between the transit frequencies of the electrons and ions and to be smaller than the electron bounce frequency

$$\omega_{te} > \omega_{be} > \omega > \omega_{t_i}.$$

For passing electrons the solution of Eq. (A2) is

$$\frac{1}{2}(g_+ + g_-)^p_e = -F_0\left(1 - \frac{\omega_{*te}}{\omega}\right)\psi, \tag{A3}$$

and for the trapped electrons

$$\frac{1}{2}(g_+ + g_-)^t_e = -F_0\left[\left(1-\frac{\omega_{*te}}{\omega}\right)\psi + \frac{\omega-\omega_{*te}}{\omega-\bar{\omega}_{De}}\overline{\left(\phi - \frac{\omega-\omega_{De}}{\omega}\psi\right)}\right]. \tag{A4}$$

The overbar denotes the bounce average defined as

$$\bar{A} \equiv \oint \frac{ds}{|v_{\|}|} A \left(\oint \frac{ds}{|v_{\|}|}\right)^{-1},$$

and the bounce average electron drift frequency depends on the energy and the velocity space pitch angle parameter κ which is defined as

$$\kappa^2 = \frac{1}{2}\left(\frac{1 - \frac{v_{\perp}^2 B_0}{v^2 B}}{\varepsilon} + 1\right).$$

For $B = B_0(1 - \varepsilon\cos\theta)$ with $\varepsilon = r/R$, the bounce averaged drift frequency reduces to

$$\bar{\omega}_{De} = 2\varepsilon_n\omega_{*e}\frac{mv^2}{T_e}\left[G_1(\kappa) + sG_2(\kappa)\right]. \tag{A5}$$

where $G_1 = -\frac{1}{2} + E(\kappa)/K(\kappa)$, and $G_2 = 2\left(G_1 - \frac{1}{2} + \kappa^2\right)$. Here, $E(\kappa)$ and $K(\kappa)$ are the complete elliptic integral of the first and second kind.

For ions we have all passing particles, we obtain

$$\frac{1}{2}(g_+ + g_-)_i = F_i\left(\frac{\omega - \omega_{*ti}}{\omega - \omega_{Di}}\right)(1-\sigma^2)^{-1}\left(\tau\phi J_0 + \frac{J_0|v_\parallel|^2}{\omega(\omega-\omega_{Di})}\frac{\partial^2}{\partial s^2}\tau\phi\right), \tag{A6}$$

where $\sigma = \frac{i|v_\parallel|}{(\omega-\omega_{Di})}\frac{\partial}{\partial s}$.

Using Eqs. (A3)–(A6) we obtain the quasi-neutrality equation

$$\left[-1-\tau+\tau P + \mathrm{TR1} - \frac{c_s^2}{\omega^2q^2R^2}\frac{\partial}{\partial\theta}P_3\frac{\partial}{\partial\theta}\right]\phi + \left[\mathrm{PS1} + \frac{c_s^2}{\omega^2q^2R^2}\frac{\partial}{\partial\theta}P_2\frac{\partial}{\partial\theta}\right]\psi = 0 \tag{A7}$$

and the parallel Ampere's law

$$\left[\mathrm{PS1} + \mathrm{TR2} + \frac{c_s^2}{\omega^2q^2R^2}\frac{\partial}{\partial\theta}P_2\frac{\partial}{\partial\theta}\right]\phi$$
$$+\left[\frac{\rho^2v_A^2}{\omega^2q^2R^2}\frac{\partial}{\partial\theta}\nabla_\perp^2\frac{\partial}{\partial\theta} - \mathrm{PS1} + \mathrm{PS2} - \frac{c_s^2}{\omega^2q^2R^2}\frac{\partial}{\partial\theta}P_1\frac{\partial}{\partial\theta}\right]\psi = 0. \tag{A8}$$

In obtaining Eqs. (A7)–(A8) we used the local approximation, i.e., $\bar{X} \cong X$. The ion kinetic integrals are given in Eq. (4) and the electron velocity integrals are given as

$$\mathrm{PS1} = \int_p d^3v\, F_0\left(1 - \frac{\omega_{*te}}{\omega}\right) \tag{A9}$$

$$\mathrm{PS2} = \int_p d^3v\, F_0\left(1 - \frac{\omega_{*te}}{\omega}\right)\frac{\omega_{De}}{\omega} \tag{A10}$$

$$\mathrm{TR1} = \int_{tr} d^3v\, F_0\frac{\omega - \omega_{*te}}{\omega - \bar{\omega}_{De}} \tag{A11}$$

and

$$\mathrm{TR2} = \int_{tr} d^3v\, F_0\left(1 - \frac{\omega_{*te}}{\omega}\right)\left(\frac{\omega_{De} - \bar{\omega}_{De}}{\omega - \bar{\omega}_{De}}\right). \tag{A12}$$

The velocity space integrations are

$$\int d^3v = \sum_{\sigma=\pm 1} \pi \int_0^\infty dv\, v^2 \int_0^h d\Lambda \frac{1}{h\left(1-\frac{\Lambda}{h}\right)^{1/2}}.$$

For passing electrons, $0 \leq \Lambda \leq h_m = 1-\varepsilon$ and for trapped electrons, $h_m \leq \Lambda \leq h(\theta) = 1+\varepsilon\cos\theta$ at given θ.

Neglecting the ion acoustic couplings Eq. (A7) and (A8) reduce to

$$\left[\frac{\omega_A^2}{\omega^2}\frac{d}{d\theta}\nabla_\perp^2\frac{d}{d\theta} + \mathrm{PS2} - \mathrm{PS1} + \frac{\mathrm{PS1}(\mathrm{PS1}+\mathrm{TR2})}{1+\tau-\tau P - TR1}\right]\psi = 0, \qquad \text{(A13)}$$

which is the generalization of Eq. (8) in the presence of trapped electrons. Solutions of Eq. (A13) are shown in Figs. 3(b) and 4(b).

References

1. W. Horton, J.E. Sedlak, D.-I. Choi, B.-G. Hong, Phys. Fluids **28**, 3050 (1985).

2. P. Similon, J.E. Sedlak, D. Stotler, H.L. Berk, W. Horton, and D. Choi, J. Comput. Phys. **54**, 260 (1984).

3. W. Horton, D.-I. Choi and B.-G. Hong, Phys. Fluids **26**, 1464 (1983).

4. C.Z. Cheng, Nucl. Fusion **22**, 773 (1982).

5. W.M. Tang, G. Rewoldt, C.Z. Cheng, M.S. Chance, Nucl. Fusion **25**, 151 (1985).

6. P. Andersson and J. Weiland, Phys. Fluids **31**, 359 (1988).

7. R.R. Dominguez and R.W. Moore, Nucl. Fusion **26**, 85 (1986).

8. G. Rewoldt, W.M. Tang and M.S. Chance, Phys. Fluids **25**, 480 (1982).

9. S.M. Kaye, R.J. Goldston, M. Bell, K. Bol, and M. Bitter, Nucl. Fusion **24**, 1303 (1984).

10. M. Nagami and the JAERI Team, D. Overskei and the GA Team, in Plasma Physics and Controlled Nuclear Fusion Research 1982 (Proc. 9th Int. Conf. Baltimore, 1982), Vol. 1, IAEA, Vienna 27 (1983).

11. M. Murakami, D.W. Swain, S.C. Bates, C.E. Bush, L.A. Charlton, J.L. Dunlap, G.R. Dyer, P.H. Edmonds, A.C. England, H.H. Haselton, J.T. Hogan, H.C. Howe, D.P. Hutchinson, R.C. Isler, T.C. Jernigan, S. Kasai, H.E. Ketterer, J. Kim, P.W. King, E.A. Lazarus, J.F. Lyon, C.H. Ma, J.T. Mihalczo, J.K. Munro, A.P. Navarro, G.H. Neilson, D.R. Overbey, V.K. Paré, M.J. Saltmarsh, S.D. Scott, J. Sheffield, J.E. Simpkins, W.L.

Stirling, C.C. Tsai, R.M. Wieland, J.B. Wilgen, W.R. Wing, R.E. Worsham, B. Zurro, in Plasma Physics and Controlled Nuclear Fusion Research 1980 (Proc. 8th Int. Conf. Brussels, 1980), Vol. 1, IAEA, Vienna 377 (1981).

12. D.-I. Choi and W. Horton, Phys. Fluids **23**, 356 (1980).

13. R.J. Hastie, K.W. Hasketh and J.B. Taylor, Nucl. Fusion **19**, 1223 (1979).

14. K.W. Hesketh, Nucl. Fusion **20**, 1013 (1980).

15. B.G. Hong, W. Horton and D.I. Choi, submitted to Plasma Physics and Controlled Fusion, 1988.

16. C.Z. Cheng, Phys. Fluids **25**, 1020 (1982).

17. K. Itoh, S.-I. Itoh, S. Tokuda, and T. Tuda, Nucl. Fusion **22**, 1031 (1982).

18. W.M. Tang, J.W. Connor and R.J. Hastie, Nucl. Fusion **20**, 1439 (1980).

19. R.J. Hastie and K.W. Hesketh, Nucl. Fusion **21**, 651 (1981).

20. B. Coppi, A. Ferreira and J.J. Ramos, Phys. Rev. Lett. **44**, 990 (1980).

21. J.W. Connor, R.J. Hastie and J.B. Taylor, Phys. Rev. Lett. **40**, 396 (1978).

Figure Captions

1. Eigenmode spectrum γ_k, ω_k from kinetic ballooning mode Eq. (9). Parameters $\varepsilon_n = 0.25, s = 1, q = 2, \tau = 1, \eta_i = 0$ and $\alpha = \beta/\beta_c = 1$ and 2. The dashed line shows the growth rate calculated from local kinetic theory with $\alpha = \beta/\beta_c = 2.0$.

2. Growth rate and frequency dependence on $k = k_\theta \rho_s$ for the same parameters as in Fig. 1 except $\eta_i = 2.0$.

3. (a) Kinetic ballooning mode growth rate dependence on beta at fixed $k = 0.5$. Parameters $\varepsilon_n = 0.25, s = 1.0, q = 2, \tau = 1$ and $\eta_i = 0$. Threshold at $\beta_K = 0.0374$ or $\alpha_1 = 0.60$. (b) Same as (a) using "$s - \alpha$" model.

4. (a) Growth rate dependence on beta for the same parameters as in Fig. 3 except $\eta_i = 2.0$. Threshold at $\beta_K = 0.006$ or $\alpha = 0.144$. (b) Same as (a) using "$s - \alpha$" model.

5. Growth rate dependence on ε_n for $k = 0.3, \beta_e = 0.046875, q = 2, \tau = 1$ and $\eta_i = 2$ with $s = 0.5$ and 1.0.

6. Growth rate dependence on shear $s = rq'/q$ for $k = 0.3, \beta_e = 0.046875, q = 2, \tau = 1$ and $\eta_i = 2$ with $\varepsilon_n = 0.1$ and 0.25.

7. Nyquist diagrams for the local electromagnetic component of the dispersion relation shown for $\eta_i = 1.0$. The contour in (a) encircles the origin twice in parts (b) and (c) and only once in part (d).

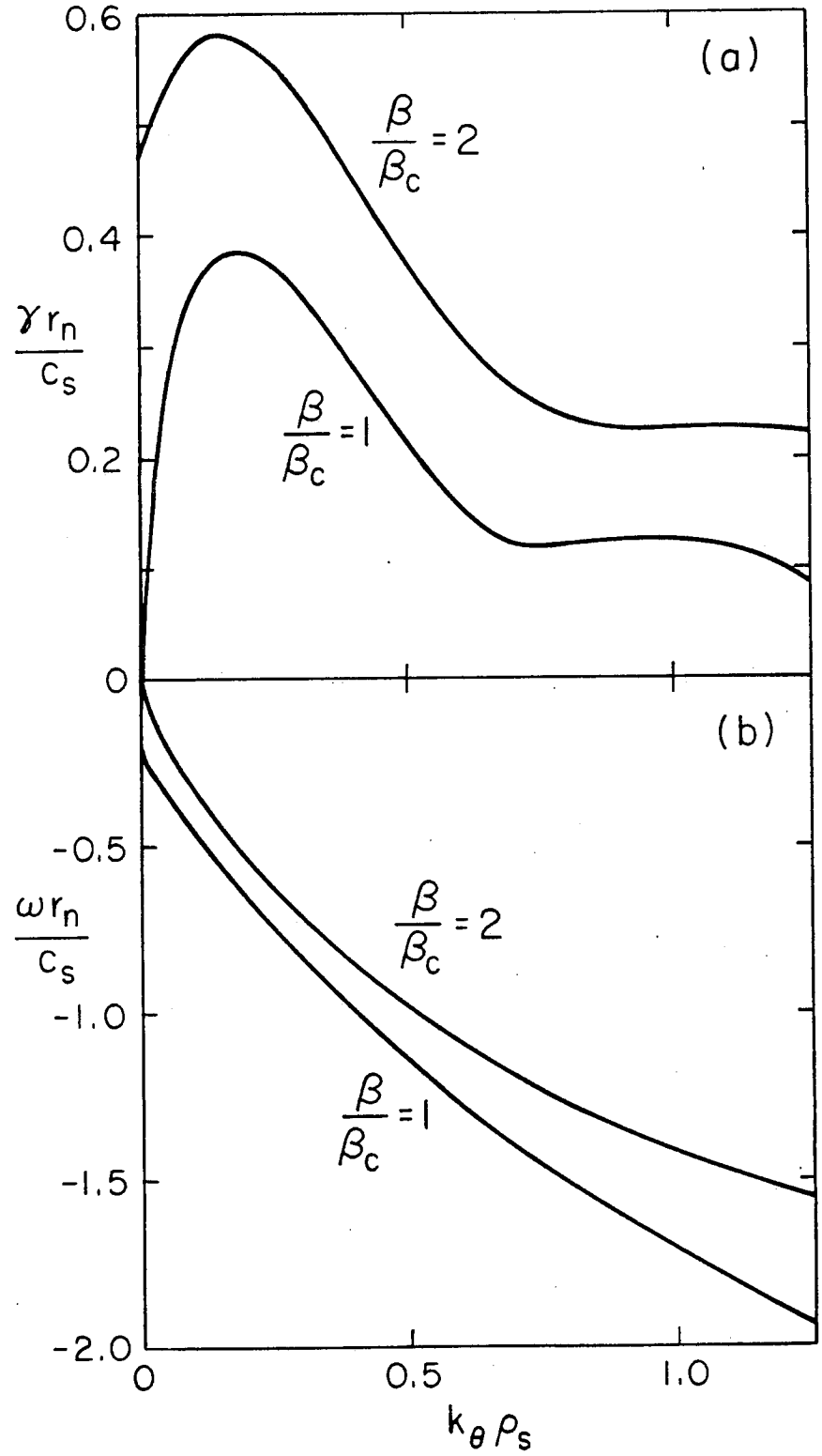
0.6
0.4
0.2
0
-0.5
-1.0
-1.5
-2.0
0
0.5
1.0
(a)
(b)
$\frac{\gamma r_n}{c_s}$
$\frac{\omega r_n}{c_s}$
$\frac{\beta}{\beta_c} = 2$
$\frac{\beta}{\beta_c} = 1$
$\frac{\beta}{\beta_c} = 2$
$\frac{\beta}{\beta_c} = 1$
$k_\theta \rho_s$

Fig. 1

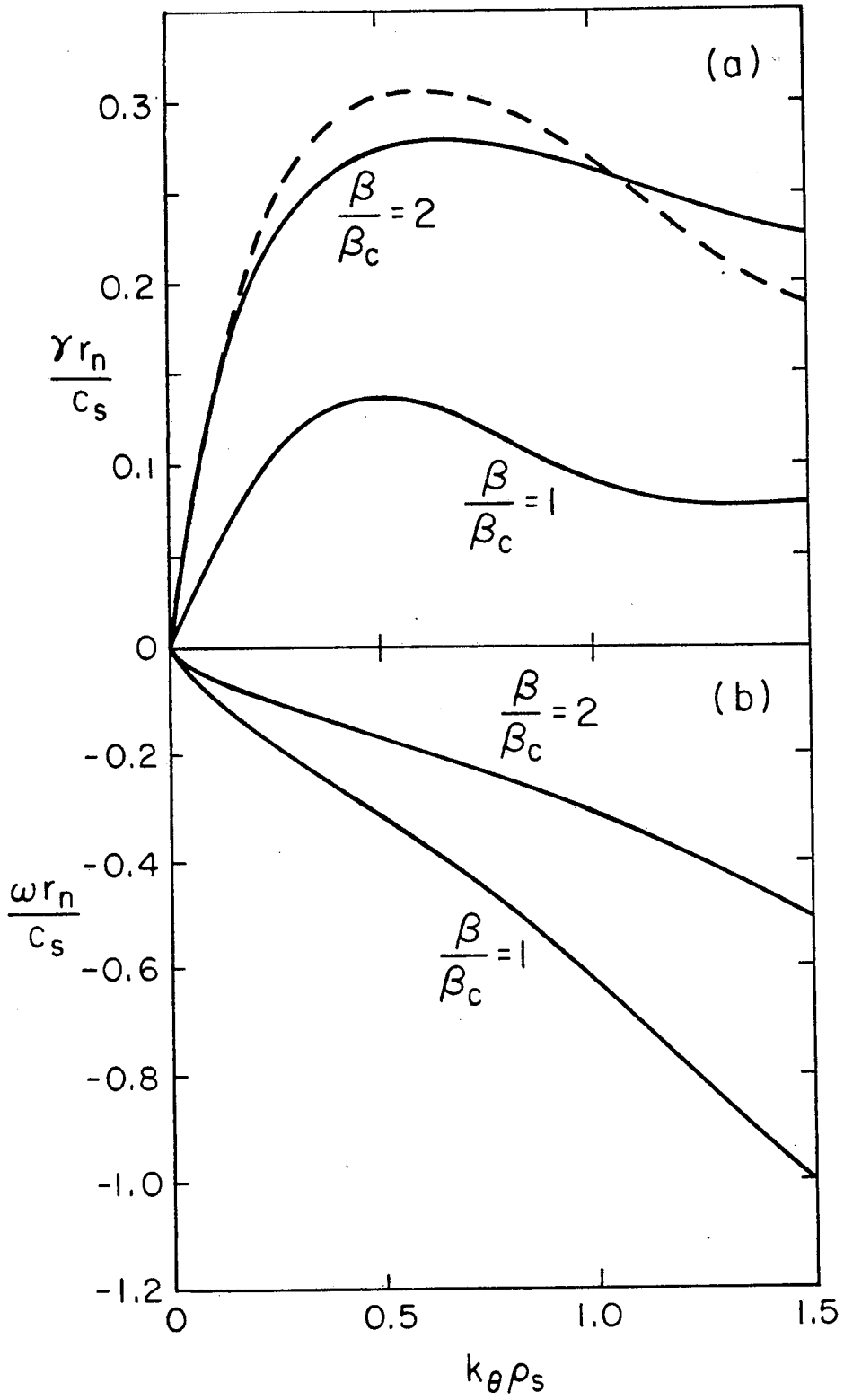
(a)
0.3
0.2
$\frac{\gamma r_n}{c_s}$
0.1
$\frac{\beta}{\beta_c} = 2$
$\frac{\beta}{\beta_c} = 1$
0
(b)
$\frac{\beta}{\beta_c} = 2$
-0.2
-0.4
$\frac{\omega r_n}{c_s}$
$\frac{\beta}{\beta_c} = 1$
-0.6
-0.8
-1.0
-1.2
0
0.5
1.0
1.5
$k_\theta \rho_s$

Fig. 2

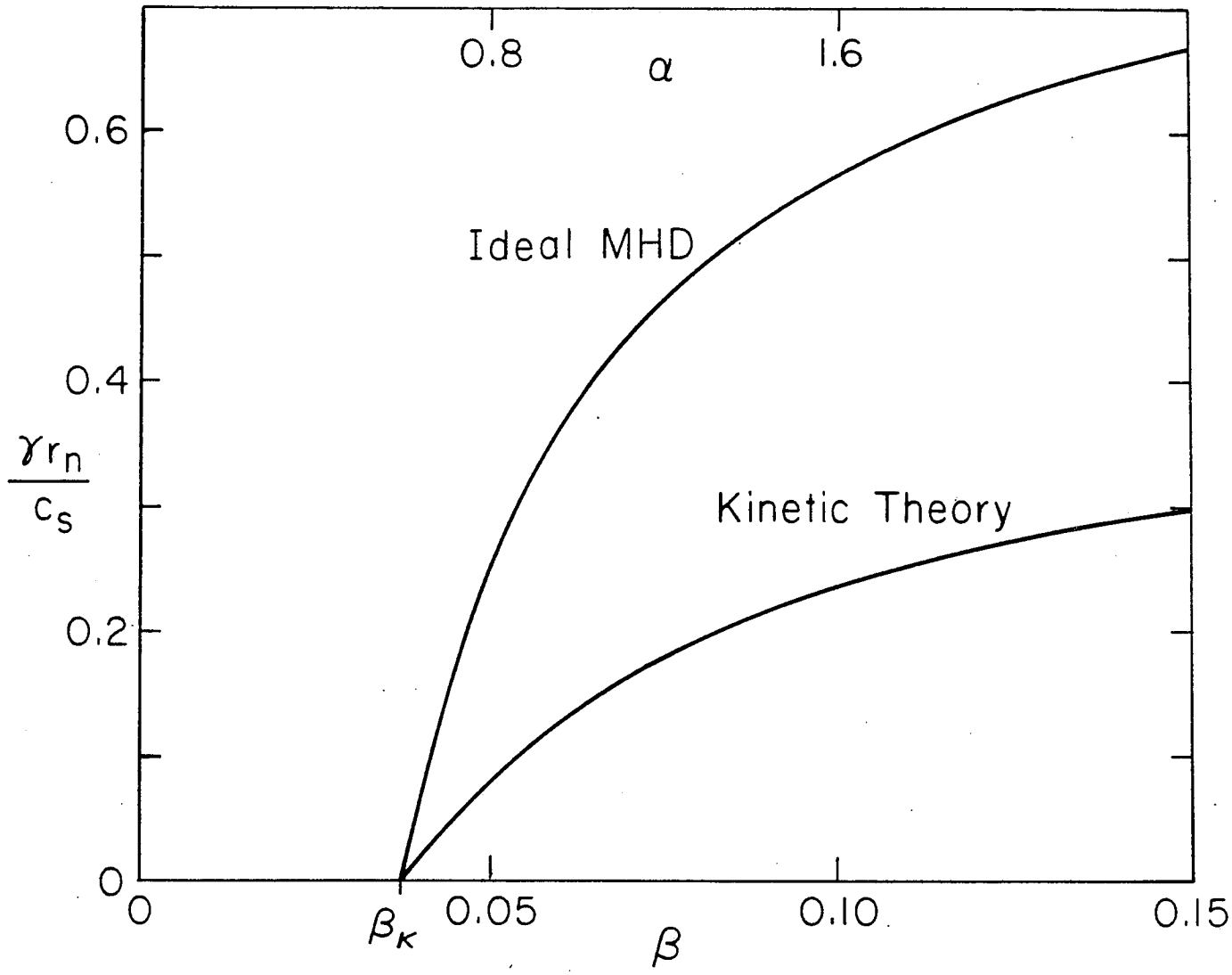
0.8
α
1.6
0.6
Ideal MHD
0.4
γr_n / c_s
Kinetic Theory
0.2
0
0
β_κ
0.05
β
0.10
0.15

Fig. 3(a)

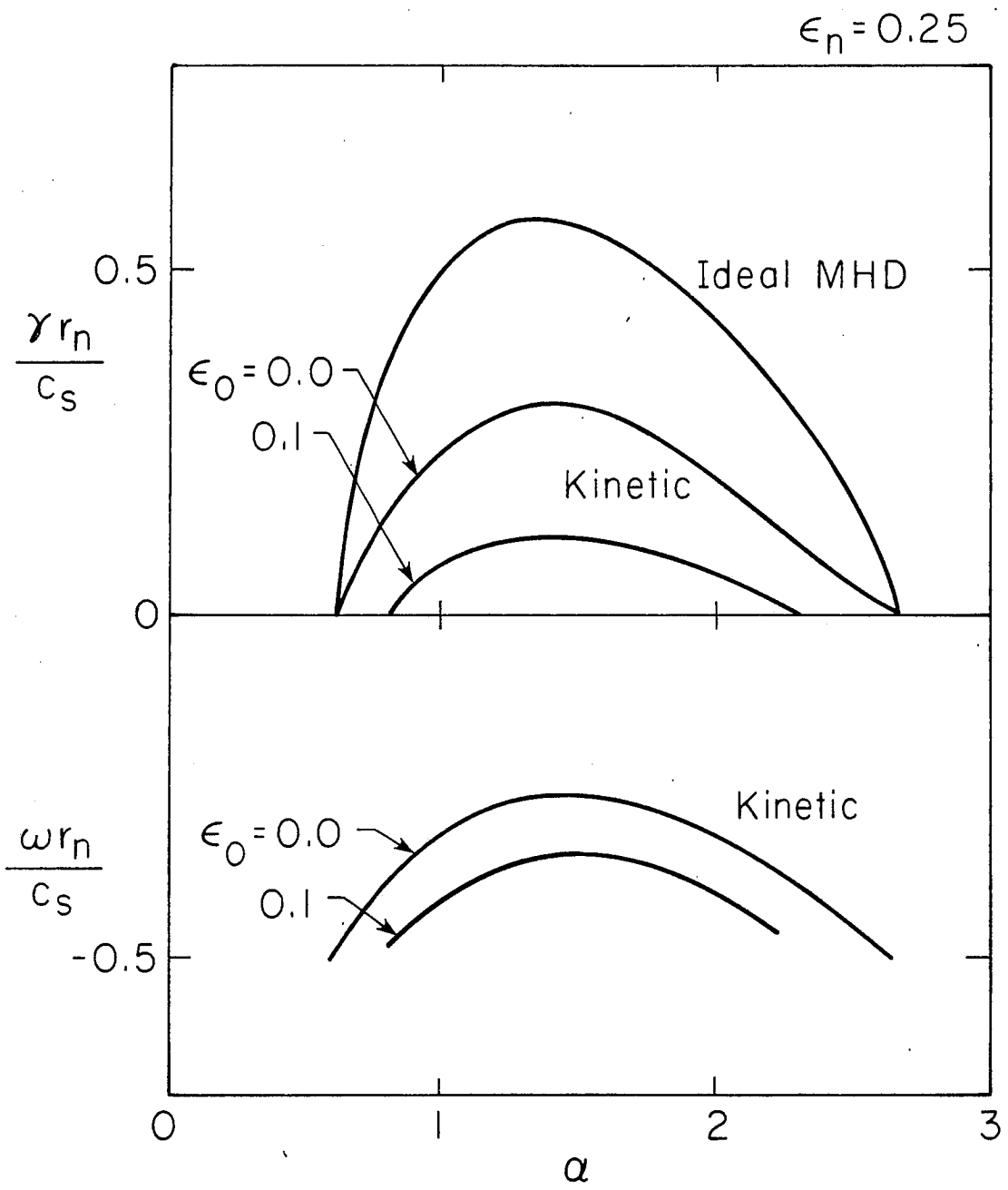
$\epsilon_n = 0.25$
0.5
$\frac{\gamma r_n}{c_s}$
$\epsilon_0 = 0.0$
0.1
Ideal MHD
Kinetic
0
$\frac{\omega r_n}{c_s}$
$\epsilon_0 = 0.0$
0.1
Kinetic
-0.5
0
1
2
3
α

Fig. 3(b)

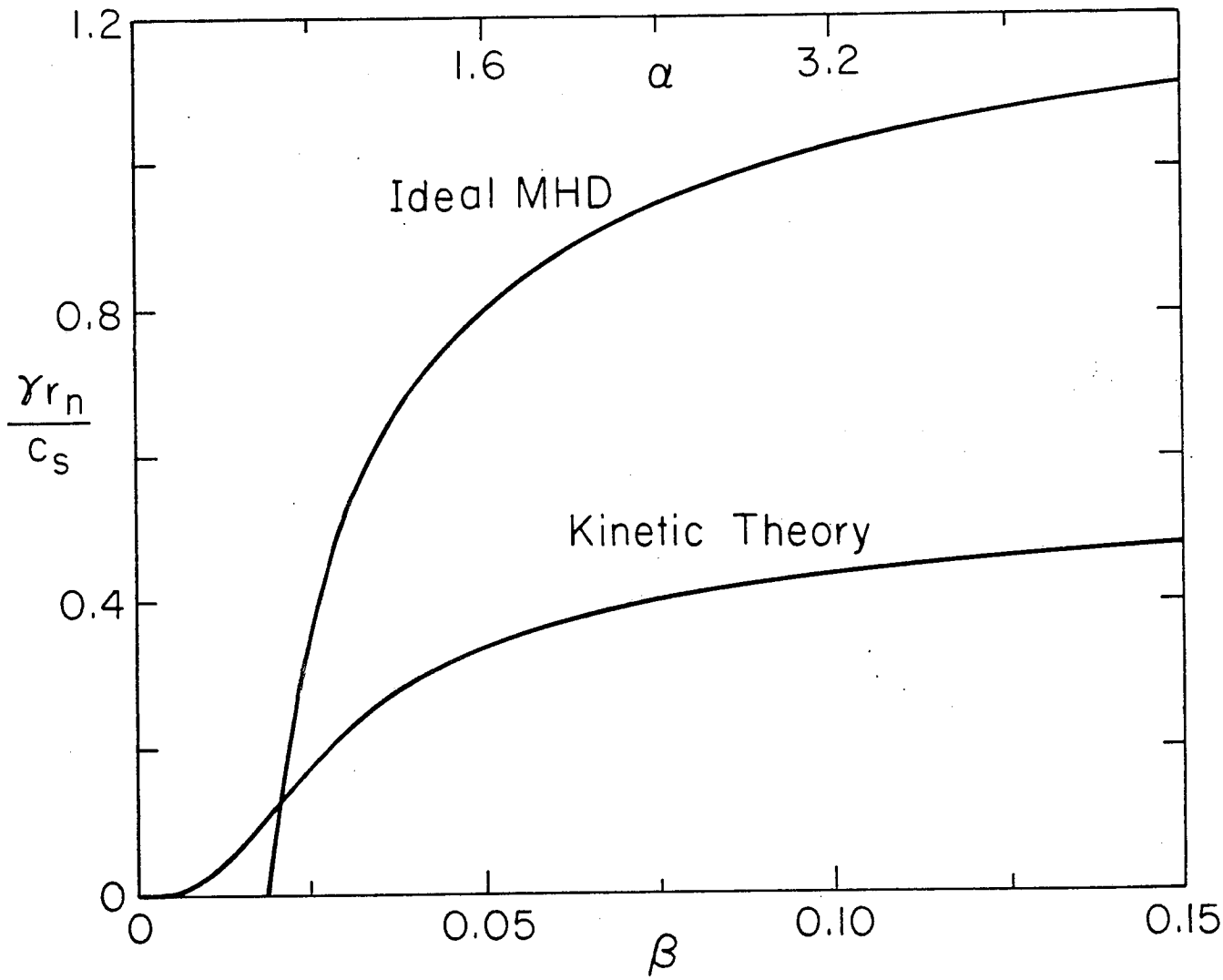

Fig. 4(a)

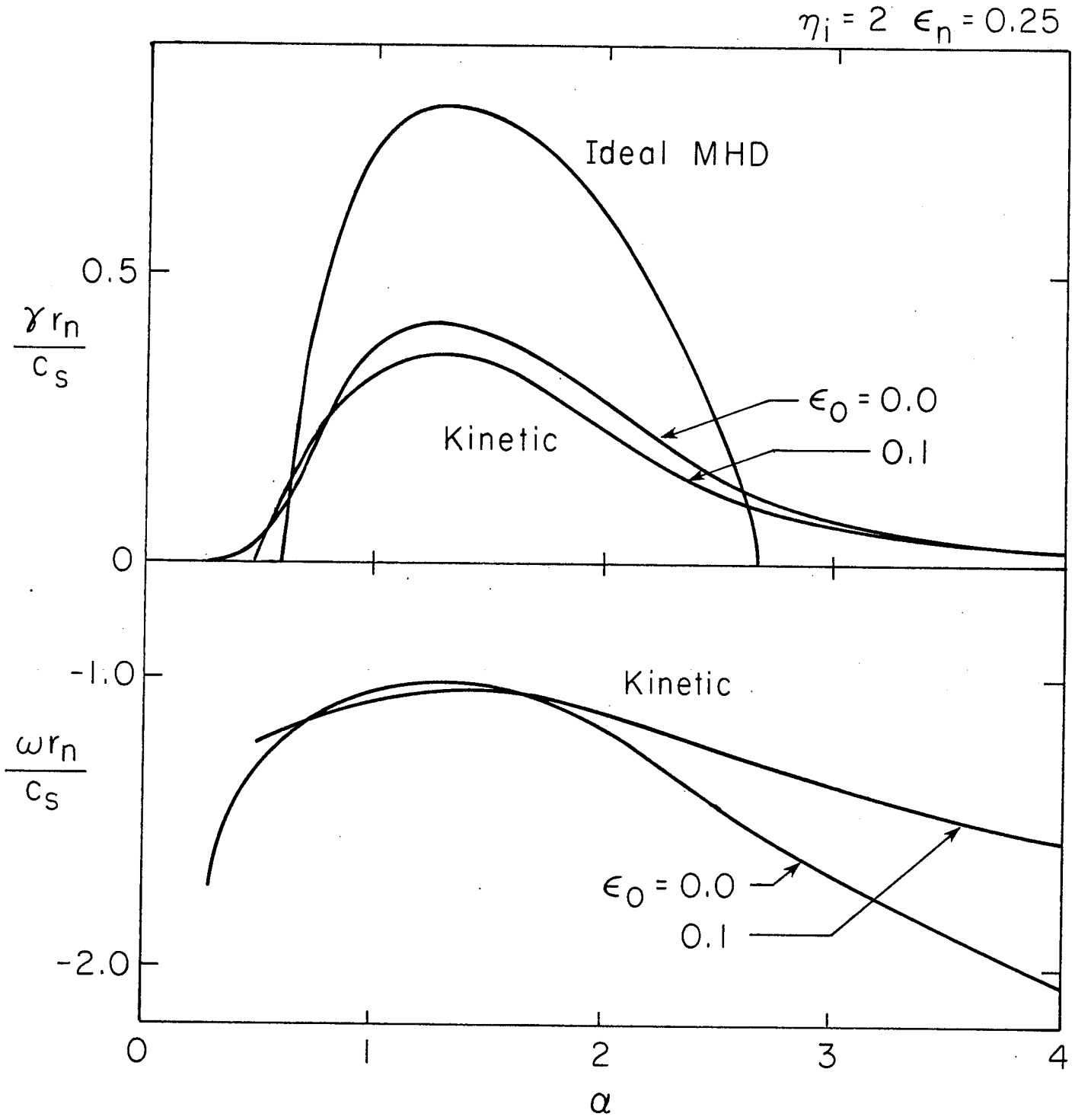
$\eta_i = 2$ $\epsilon_n = 0.25$
Ideal MHD
Kinetic
$\epsilon_0 = 0.0$
0.1
$\frac{\gamma r_n}{c_s}$
0.5
0
-1.0
-2.0
Kinetic
$\epsilon_0 = 0.0$
0.1
$\frac{\omega r_n}{c_s}$
0
1
2
3
4
α

Fig. 4(b)

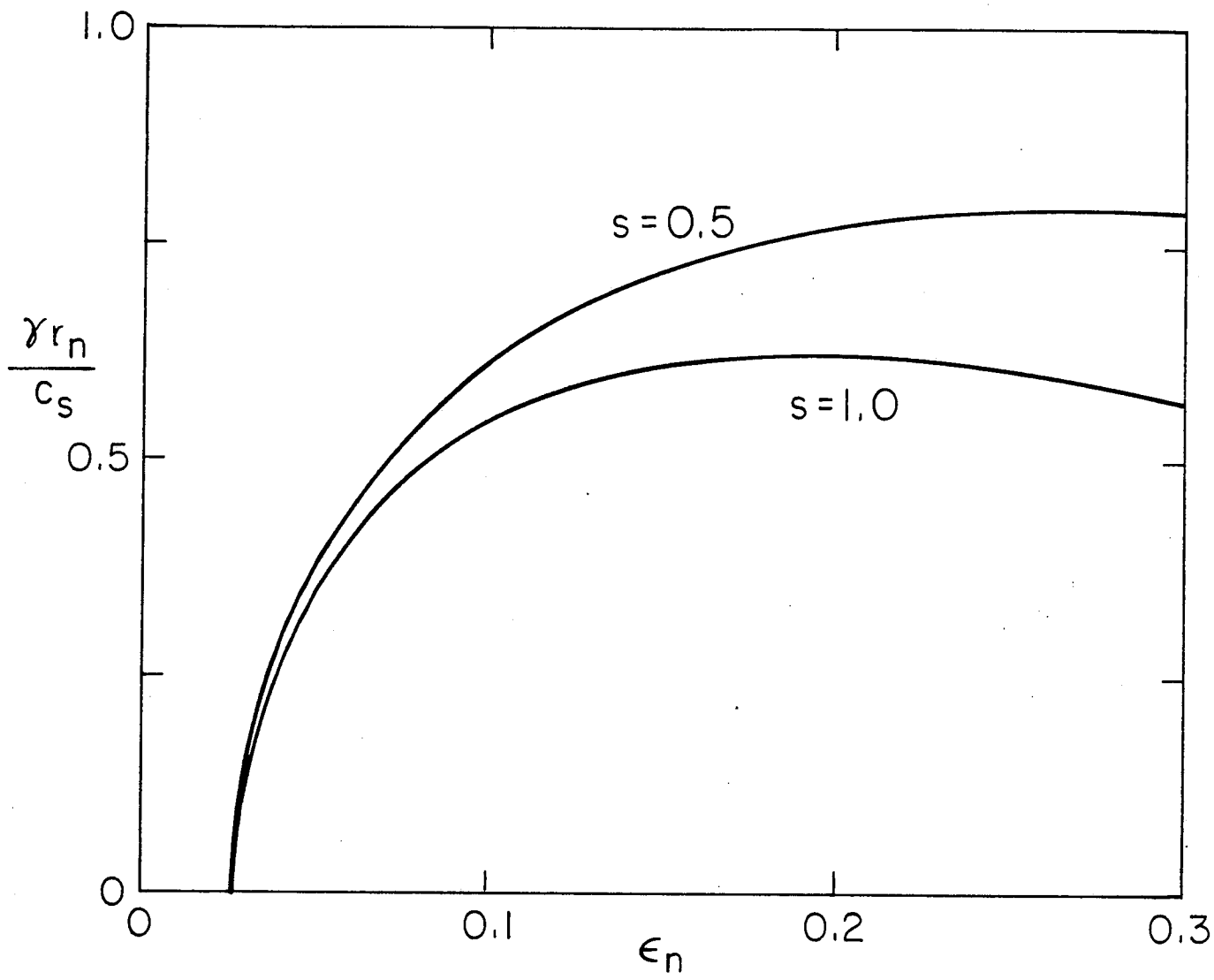

Fig. 5

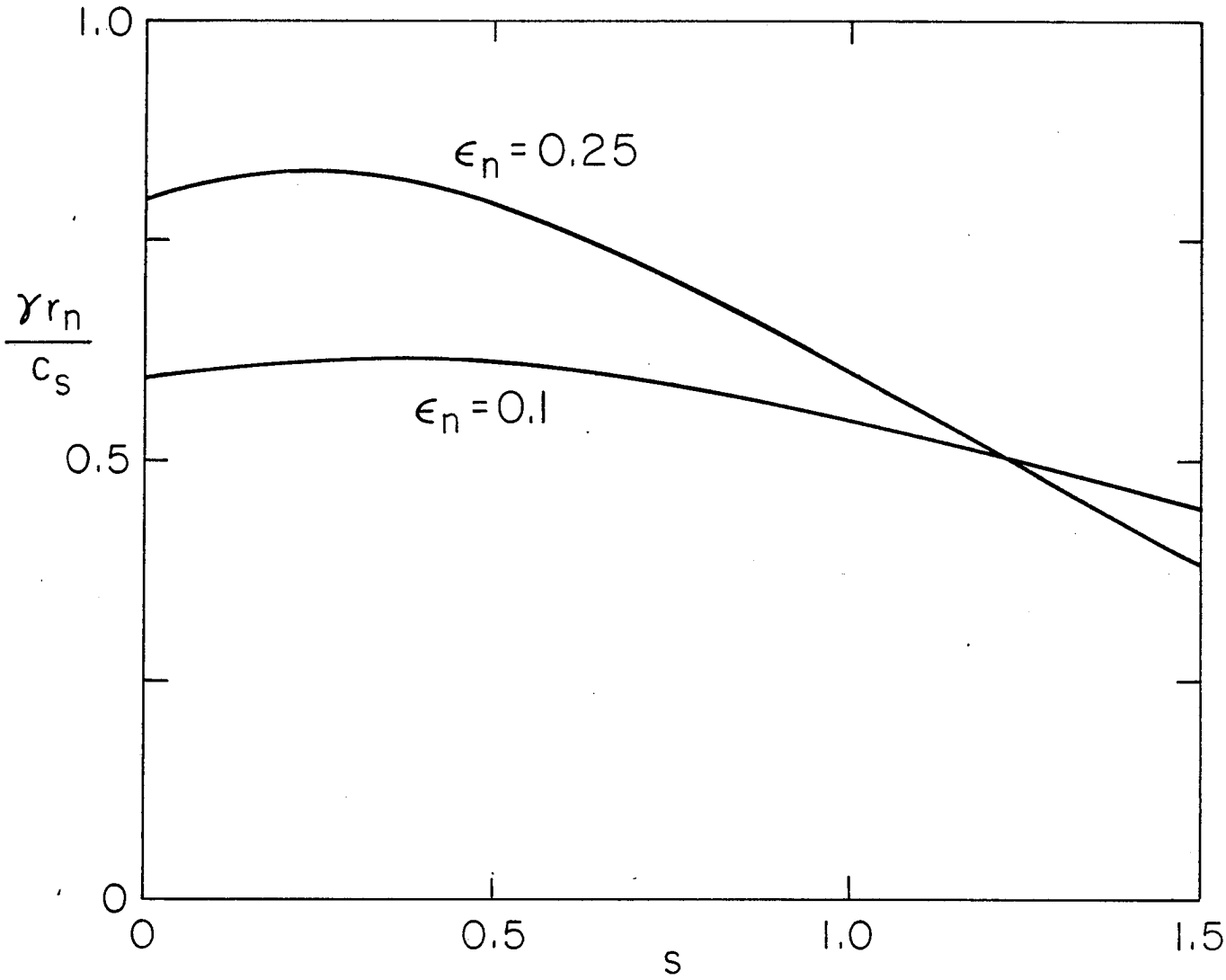

Fig. 6

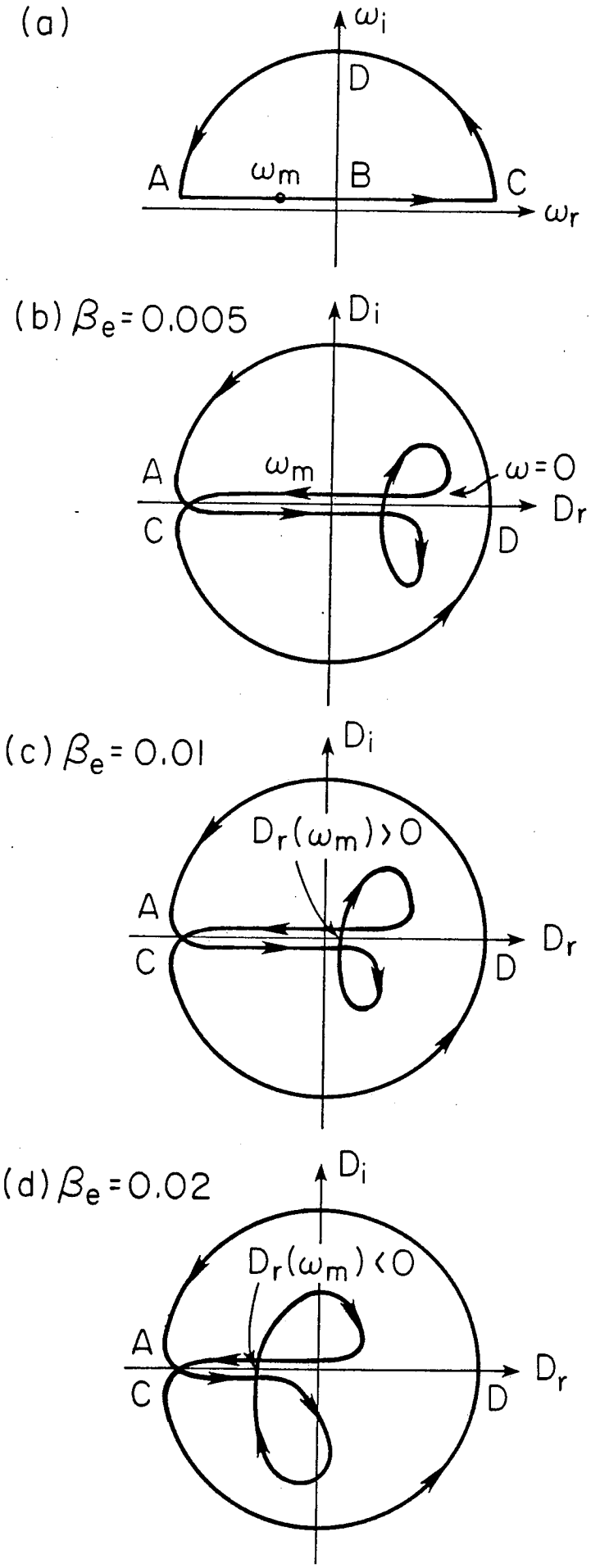
(a)
ω_i
D
A
ω_m
B
C
ω_r
(b) $\beta_e = 0.005$
D_i
A
ω_m
$\omega = 0$
D_r
C
D
(c) $\beta_e = 0.01$
D_i
$D_r(\omega_m) > 0$
A
D_r
C
D
(d) $\beta_e = 0.02$
D_i
$D_r(\omega_m) < 0$
A
D_r
C
D

Fig. 7